Pharm Res (2012) 29:1518–1529
DOI 10.1007/s11095-011-0648-6

RESEARCH PAPER

Population Pharmacokinetic/Pharmacodynamic Model for the Sedative Effects of Flibanserin in Healthy Volunteers

Iñaki F. Trocóniz • Katja Boland • Alexander Staab

Received: 17 August 2011 / Accepted: 5 December 2011 / Published online: 5 January 2012

ABSTRACT

Purpose Flibanserin is being developed for treating hypoactive sexual desire disorder in women; the main side effect is sedation. The analysis objective was to relate flibanserin plasma concentrations with acute sedative effects using a population pharmacokinetic/pharmacodynamic (PK/PD) model.

Methods The population model was developed with NONMEM based on data from 24 healthy volunteers. "Drowsiness" was serially assessed by a Visual Analogue Scale (VAS) on a baseline day and after morning oral administration of 100 mg flibanserin together with PK sampling.

Results PK was best described by a three-compartment disposition model and transit compartments accounting for the lag time in absorption. VAS "drowsiness" baseline profiles were modeled using linear splines with three breakpoints located at clock times at first and last observation, and at the median of the observation time across subjects. The drug effect followed a sigmoidal E_{MAX} model using predicted effect site concentrations (C_e). The VAS *vs.* C_e relationship was very steep and effect site and plasma concentration-time profiles were very similar thus suggesting little delay between the occurrence of maximum flibanserin plasma concentrations and drowsiness.

Conclusions At effect site concentrations lower than ~200 ng/mL that are reached approximately 4 h after administration, flibanserin shows hardly any effect on the VAS "drowsiness" scale.

I. F. Trocóniz (✉)
Department of Pharmacy and Pharmaceutical Technology
School of Pharmacy, University of Navarra
Pamplona 31080, Navarra, Spain
e-mail: itroconiz@unav.es

K. Boland • A. Staab
Translational Medicine, Boehringer Ingelheim
Pharma GmbH & Co KG
Biberach, Germany

KEY WORDS flibanserin · NONMEM · PKPD modeling · sedation

ABBREVIATIONS

-2LL	-2xlog likelihood
36NPDE	normalized prediction distribution errors
AEs	adverse events
AIC	Akaike information criteria
C_e	predicted effect site concentration
ckt	clock time
CL	total plasma clearance
CL_{D2} CL_{D3}	inter-compartmental clearances
F	absolute bioavailability
$f(C_e)$	pharmacodynamic model
HSDD	hypoactive sexual desire disorder
k_{1e}	1st order rate constant of distribution from the central compartment to the biophase compartment
k_A	1st order rate constant of absorption
k_{e0}	1st order rate of elimination from the biophase
k_{TR}	1st order rate constant of transit
NONMEM	non-linear mixed effects model
NPC	numerical predictive checks
NPDE	normalized prediction distribution errors
PK/PD model	pharmacokinetic/pharmacodynamic model
$T_{1,..N}$	transit compartments
V_1, V_2, V_3	apparent volumes of distribution of the central, peripheral shallow and peripheral deep compartments, respectively
VAS	visual analogue scale

INTRODUCTION

A significant percentage of the women diagnosed with sexual dysfunction suffer from Hypoactive Sexual Desire

Disorder (HSDD) which is associated with psychological distress affecting quality of life (1,2). Currently there is no approved pharmacotherapy available to treat HSDD, and therefore a medical need exists for the development of novel therapies.

Flibanserin (BIMT 17 BS) is a cortical, post-synaptic full serotonin (5-HT)$_{1A}$ agonist and a 5-HT$_{2A}$ antagonist (3), which was developed for the treatment of women with HSDD (4,5). Flibanserin also binds with moderate affinity to the dopamine D4, 5-HT2B, and 5-HT2C receptor (6).

In humans, flibanserin is rapidly absorbed after oral administration and shows an absolute bioavailability (F) of approximately 33% mainly due to first pass metabolism through the liver (7). Flibanserin is highly protein bound (98%) and is mainly metabolized by the cytochrome P450 isoform 3A4. After administration of a single [^{14}C] labelled oral dose, flibanserin related material was found in urine and feces in approximately equal amounts. After intravenous administration of flibanserin, total plasma clearance (CL) and volume of distribution (V) were 26 L h^{-1} and 186 L, respectively. The terminal half-life at steady-state was approximately 10 h. These results were obtained by non-compartmental pharmacokinetic (PK) analyses (7).

In clinical pharmacology studies, the highest tested dose was 100 mg t.i.d. The incidence of adverse events (AEs) in premenopausal women with HSDD taking flibanserin was low and the majority of adverse events were mild to moderate in severity. The frequently occurring events were dizziness, nausea, fatigue, and somnolence at approximately 10–12% and insomnia at approximately 5% (7).

Sedative type side effects were usually most prominent in the time frame between 1 and 4 h after dosing; thus, their occurrence appeared to be related directly to the time of maximum flibanserin plasma concentrations (7), which provides the opportunity to quantify this observation using a model based approach.

Based on the above considerations, the main objective of the present analysis was to further characterize the PK characteristics of flibanserin and to describe the relationship between the plasma concentrations and a standardised assessment of "drowsiness". Furthermore, the measure of drug exposure that is best correlated with drowsiness should be identified, and if possible a drug exposure threshold below which a low incidence drowsiness occurs should be determined. The result of that analysis was a population model that allows to predict the incidence of clinically significant changes in drowsiness induced by flibanserin under different clinical scenarios (i.e., different dose levels, dosing schemes or absorption rates) that might be potentially explored during further clinical development of flibanserin.

METHODS

Patient Population and Study Design

Data from two different phase I clinical trials were used. Subjects either received flibanserin as an intravenous infusion (IV study), or as an oral immediate release tablet (PO study). The data from the IV study was used to develop the flibanserin disposition model.

All participants provided written informed consent consistent with International Conference on Harmonization of Technical Requirements for Registration of Pharmaceuticals for Human Use—Good Clinical Practice (ICH–GCP) and local legislation, once the nature and the intention of the investigation were fully explained. The studies were performed in accordance with the Declaration of Helsinki and were approved by the institutional review board of the ethics committee at each study site.

Inclusion criteria: Healthy volunteers were enrolled in the study as determined by the results of screening based upon a complete medical history, including the physical examination, vital signs, 12-lead ECG, clinical laboratory tests, and age between 21 and 50 years with a body mass index between 18.5 and 29.9 kg/m^2 or a Broca index ±20% of the normal range.

Main exclusion criteria were a disease or observed abnormality of clinical relevance, e.g. gastrointestinal, hepatic, renal, respiratory, cardiovascular, metabolic, immunological, hormonal, central nervous system, or psychiatric disorders; relevant gastrointestinal tract surgery; smoking (more than 10 cigarettes or 3 cigars or 3 pipes per day); drug and/or alcohol abuse; positive pregnancy test; excessive physical activities or blood donation prior to the study, and participation in another trial with an investigational drug within 2 months prior to administration or during the trial.

IV Study

Flibanserin at dose levels of 0.5, 1, 2, 5, 10, and 20 mg was administered to 12 healthy male volunteers by a 30 min intravenous infusion. Each subject received three of these doses separated by a washout period of 2 to 3 weeks, thus, always six volunteers were treated per dose level.

Blood samples for determination of flibanserin in plasma were taken pre-dose, 10, 20, 30, 35, 40, 50 min, 1.25, 1.5, 3, 6, 9, 12, 15, 24, 32, and 48 h after start of infusion. Data from this study were used in support of the PK model development for flibanserin.

PO Study

This study was a single-centre, open-label trial in which, amongst other formulations, flibanserin was administered

orally as an immediate release tablet at the dose of 100 mg to 24 healthy volunteers (14 males and 10 females). The immediate release treatment period from which the data were included for PK/PD modeling consisted of two study days. On first day (baseline day), sedative effects were captured by the Visual Analogue Scale (VAS) "drowsiness" at the same clock times of the day as scheduled on the treatment day. On the second day (treatment day), the subjects received the flibanserin 100 mg immediate release tablet with ~240 mL water in the time window between 7:00 and 9:00 in the morning after an overnight fast. VAS response and blood samples for determination of flibanserin in plasma were obtained pre dose and approximately at 15, 30, 45 min and 1, 1.5, 2, 3, 4, 6, 8, 10, 12, and 24 h after drug administration. VAS measurements were always recorded before blood sampling.

VAS "Drowsiness"

At each measuring time point, the volunteers assessed their subjective impression of "drowsiness" by means of a VAS. The volunteers were asked to mark an adequate position on a line between the two limits "not in existence" and "very strong". The length of the line was exactly 10 cm, and the investigator or a designee determined the score (values between 0 = "not in existence" and 10 = "very strong") by measuring the distance in cm from the beginning of the line (position "not in existence") to the position marked by the subject. Data were not rounded to the closest natural value. The total scale had 101 possible values. The score was written down on the case report form by the site personnel.

Determination of Flibanserin Concentrations in Plasma

In the PO study, flibanserin was analyzed in human plasma by Boehringer Ingelheim with a validated high performance liquid chromatography coupled to tandem mass spectrometry (HPLC-MS/MS) method using deuterated internal standard, [D8]flibanserin. Samples were purified by solid-phase extraction. Chromatography was conducted on an analytical C18 reversed-phase column with isocratic elution. The analyte was detected and quantified with MS/MS using electrospray ionization in the positive ion mode. A linear calibration curve was obtained over the concentration range from 1 to 1,000 ng/mL of flibanserin using a plasma volume of 50 μL. The lower limit of quantification was 1 ng/mL. Within study bias and precision of the assay was below 6% and 3%, respectively. In the IV study, flibanserin plasma concentrations were determined after liquid/liquid extraction by a HPLC method with ultra-violet (UV) detection at 210 nm using a flibanserin analog as internal standard. The calibration range of this method was 2–1,000 ng/mL, 2 ng/mL being the lower limit of quantification. The variability for concentrations below 10 ng/mL was <12.5% and <7.5% for concentrations greater than 10 ng/mL, the assay bias was below 6.5%.

Data Analysis

The population approach was applied for all analyses using the software NONMEM version VI (8) with the first order conditional estimation (FOCE) method with INTERACTION. Inter-subject and inter-occasion (9) variability (ISV, and IOV) were modeled exponentially. Prior to the analysis the PK and PD observations were logarithmically transformed. Plasma concentrations below the limit of quantification were ignored. Residual variability was described with an additive error in the log domain for PK and PK/PD data. During the development of the PK/PD model for flibanserin effects on VAS "drowsiness," the PK data were analyzed first and then the response data were fitted using the individual pharmacokinetic parameter model estimates. It was not possible to fit the PK and PD data simultaneously as the models did not terminate successfully and did not provide estimates for model parameters.

Model Selection

Selection between models was based mainly on the inspection of goodness-of-fit plots including conditional weighted residuals, CWRES (10), and the precision of the parameter estimates. The minimum value of the objective function provided by NONMEM that is approximately equal to −2xlog likelihood (−2LL), served as a guide during model building. For two nested models a decrease in −2LL of 6.63 points for an added parameter, corresponding to a p-value of 0.01, was regarded as a significant improvement of the model. For non-nested models the Akaike information criteria, AIC (11), calculated as AIC = −2LLx2xNP, where NP is the number of parameters in the model, was used for selection between models. Model parameter estimates were presented together with the corresponding relative standard error [RSE(%)], as a measure of parameter imprecision, which were computed from the results obtained from the covariance step in NONMEM. The degree of ISV was expressed as coefficient of variation [CV(%)].

Model Evaluation

Parameter precision for the parameters of the final PK and PK/PD model was further evaluated computing the 2.5th, 50th, and 97.5th percentiles obtained from the analysis of two hundred bootstrap datasets. The bootstrap analysis was performed using Perl-speaks-NONMEM (12).

Model performance was further evaluated by exploring normalized prediction distribution errors, NPDE (13), and

numerical predictive checks (NPC). For both, NPDE and NPC, five hundred datasets with the same study design characteristics as the original studies were simulated. For each dataset the medians of the individual maximum concentration (C_{MAX}), AUC_{last} (area under the concentration *vs.* time curve between 0 and last time of measurement), $VAS_{MAX\_Day\ 1}$ (cm), maximum VAS score at day 1 (baseline day), $VAS_{MAX\_Day\ 2}$ (cm), Maximum VAS score at day 2 (treatment day), and % Δ VAS >2 cm, percentage of subjects showing a difference greater than 2 cm in the maximum increment in VAS response between treatment and baseline days were calculated. Then the 5th, 50th, and 95th percentiles of the overall median distribution were computed, and compared with the 50th percentiles obtained from the raw data.

Pharmacokinetic Modeling

Data from the IV and PO studies were analyzed simultaneously. Disposition of flibanserin in plasma was analyzed by compartmental models parameterized in apparent volumes of distribution, elimination- and distribution clearances. Different absorption models (14) including transit compartment models (15) were evaluated to describe drug input.

Pharmacokinetic/Pharmacodynamic Modeling

The following steps were followed to establish the PK/PD VAS effects model.

Step 1: Baseline Model. To develop the baseline model, the data obtained at the baseline day were used. A visual inspection revealed that, within a subject, the VAS data did not remain at a constant value over time during a day. In addition, the way the VAS data varied with clock time (ckt) did not suggest a clear trend across subjects or occasions. Therefore an empirical model based on linear splines was developed.

A linear spline is characterized by a number of real numbers called breakpoints and a number of polynomials, which simply join at the breakpoints (16). Number and locations of the breakpoints were selected as a part of the model building process, and the heights of the spline at each of the breakpoints were the model parameters to be estimated. With regard to location, two approaches were explored: (a) breakpoints located at equally spaced clock times, and (b) breakpoints located at different sets of percentiles of clock times. The predicted VAS scores were constrained to be in the interval between 0 and 10. In the following expressions, a baseline model including an internal breakpoint located at the 50th percentile of the clock time distribution ($ckt_{50}th$) is represented.

First, variables TP1, TP2, and TP3 were defined as follows:

$$TP1 = \log\left(\frac{H_{0^{th}}}{1-H_{0^{th}}}\right);\quad TP2 = \log\left(\frac{H_{50^{th}}}{1-H_{50^{th}}}\right);\quad TP3 = \log\left(\frac{H_{100^{th}}}{1-H_{100^{th}}}\right) \tag{1}$$

where H_0^{th}, H_{50}^{th}, and H_{100}^{th} represent the population heights (parameters to be estimated) at the breakpoints located at the 0^{th}, 50^{th}, and 100^{th} percentiles of the clock time distribution, ckt_0^{th}, ckt_{50}^{th}, and ckt_{100}^{th}, respectively. H_0^{th}, H_{50}^{th}, and H_{100}^{th} were constrained between 0 and 1. To constrain the individual model predicted heights at the breakpoints (H1, H2, and H3) between 0 and 1 the following transformation was used:

$$H1 = \frac{e^{TP1+\eta_1}}{1+e^{TP1+\eta_1}};\quad H2 = \frac{e^{TP2+\eta_2}}{1+e^{TP2+\eta_2}};\quad H3 = \frac{e^{TP3+\eta_3}}{1+e^{TP3+\eta_3}} \tag{2}$$

where η_{1-3} represent random effects with mean 0 and variance ω_{1-3}^2, respectively.

Individual predicted heights at times different from the location of breakpoints were obtained by linear interpolation.

Finally the predicted baseline VAS value ($VAS_{Base,ckt}$) in logarithmic scale at any given clock time was obtained based on the following algebraic expressions:

$$\begin{aligned}&\log(VAS_{Base,ckt}) = \log\left(10 \times \left[H1 + \left(\frac{H2-H1}{ckt_{50^{th}}-ckt_{0^{th}}}\right) \times (ckt - ckt_{0^{th}})\right]\right)\\ &\text{for } (ckt_{0^{th}} \le ckt < ckt_{50^{th}})\\ &\log(VAS_{Base,ckt}) = \log\left(10 \times \left[H2 + \left(\frac{H3-H2}{ckt_{100^{th}}-ckt_{50^{th}}}\right) \times (ckt - ckt_{50^{th}})\right]\right)\\ &\text{for } (ckt_{50^{th}} \le ckt < ckt_{100^{th}})\end{aligned} \tag{3}$$

Step 2: Drug Effect Model. The VAS data obtained during the baseline and treatment days were fitted simultaneously to select the drug effect model. The baseline base model established in step I was used, but parameters were re-estimated. Linear and non-linear drug effect models were assessed for their ability to describe the relationship between the plasma concentration in the central compartment (C_P), the effect site concentration,C_e, (17) and the VAS data. The equation below shows the model structure of a sigmoidal E_{MAX} model based on C_e to describe drug effects observed at certain clock times (VAS_{ckt}) in logarithmic scale:

$$\begin{aligned}&\log(VAS_{ckt})\\ &= \log\left[VAS_{Base,ckt} + (10 - VAS_{Base,ckt}) \times \left(\frac{C_e^{\gamma}}{C_e^{\gamma} + C_{50}^{\gamma}}\right)\right]\end{aligned} \tag{4}$$

where C_{50} is the predicted C_e at half-maximal VAS response [10-$VAS_{Base,ckt}$], and γ is the parameter governing the steepness of the VAS *vs.* C_e curve. The right hand of Eq. 4 resembles a sigmoidal E_{MAX} model in which E_{MAX}

instead of being estimated was substituted by the maximal score 10 minus the baseline score. This parameterization was used to prevent the predicted response to be greater than the maximum score, regardless of the VAS score at baseline.

During model building the logistic transformation was also explored resulting in a worse description of the data (−2LL increased in more than 100 points with respect the selected model). The logit (L) had the form of $L = VAS_{Base,ckt} + f(C_e)$, where $VAS_{Base,ckt}$ had the same structure as described above (3) without the need of constraints for H^{th}_{0-100}, and H1-3, and f (C_e) represents a linear or non-linear (E_{MAX}, or sigmoidal E_{MAX}) model describing drug effects.

In the current analysis only the impact of sex on the PK and PD parameters was investigated.

Model Simulations

To explore the relationship between C_{MAX} and drowsiness effects of flibanserin, five hundred studies of the same design characteristics as the original PO study were simulated using the selected PK/PD model, and various first order absorption rate constants (K_A): 1.61, 0.8, 0.4, 0.2 and 0.1 h^{-1}. For each of the simulated datasets the median of the individual C_{MAX} values and the percentage of subjects showing a difference greater than 2 cm in the maximum increment in VAS response between baseline and treatment day (% ΔVAS >2 cm) were calculated. The definition of a clinically significant change in drowsiness as a maximum increase in the VAS score of greater than 2 cm was chosen by analogy to analyses of VAS scores for pain (18).

RESULTS

The PK model was developed with a total of 729 plasma concentrations (n=404, IV study; n=325, PO study) obtained from 12 to 24 volunteers, respectively.

A total of 647 VAS observations from 24 subjects participating in the PO study were used to establish the final PK/PD model; 335 were obtained at baseline day, and 312 during the treatment day.

Pharmacokinetic Modeling

Flibanserin disposition in plasma was best described with a three-compartment model. ISV was included for CL, distribution clearance between the central and shallow peripheral compartment (CL_{D2}), and the apparent volume of distribution of the shallow peripheral compartment (V_2). Flibanserin showed linear PK characteristics for the two administration routes and over the dose range studied. An oral absorption model including a series of transit compartments provided a better fit compared to a model with only a first order rate absorption. The data supported the incorporation of ISV on k_A, MTT, mean transit time, and NTC, number of transit compartments, but not on the absolute bioavailability that was found to be lower than 100% and was estimated to be 45.9%. Covariance between ISV and the presence of IOV were non-significant ($p>0.05$). Residual variability was described with an additive random-effect model in the logarithmic scale, and the estimation of different magnitudes of the residual variability between the IV and PO studies was not supported by the data. Figure 1 shows a schematic representation of the selected PK model. Sex did not show significant covariate effect in any of the PK parameters ($p>0.05$).

Table I lists the estimates of the population PK model. ε-shrinkage was 11%, and η-shrinkage corresponding to CL, CL_{D2}, V_2, k_A, MTT, and NN was 7, 7, 22, 8.4, 5.1, and 26%, respectively (19). All parameters were estimated with adequate precision. Results from the bootstrap analyses provided median values of the parameters that were very close to the NONMEM estimates, and the 95% confidence intervals did not include the value of zero for any of the parameters in the model. Figure 2 showing the goodness of fit plots with the results from the NPDE, indicates that the model perfomed properly for the intravenous and oral data. Similar results were obtained from the NPC (see Table II). The two descriptors (C_{MAX} and AUC_{last}) calculated from the raw data at each dose level fell within the 90% prediction intervals calculated from the simulated studies except for AUC_{last} for the lowest intravenous dose.

Pharmacokinetic/Pharmacodynamic Modeling

Baseline Model

A model including three breakpoints located at the clock time of the first observation, the clock time corresponding to the median of the observation time across subjects, and the clock time of the last observation (6.65, 10.77, and 21.1 h, respectively), was initially fitted to the baseline VAS *vs.* clock time data. ISV was introduced for each of the height parameters and residual variability was modeled using an additive variability model. Increasing the number of breakpoints and locating them at the different percentiles of the clock time distribution did not result in a better fit.

Drug Effect Model

A decrease of approximately 100 points in −2LL was obtained when drug effects were modeled using an E_{MAX} model based on C_P, compared to a model in which drug

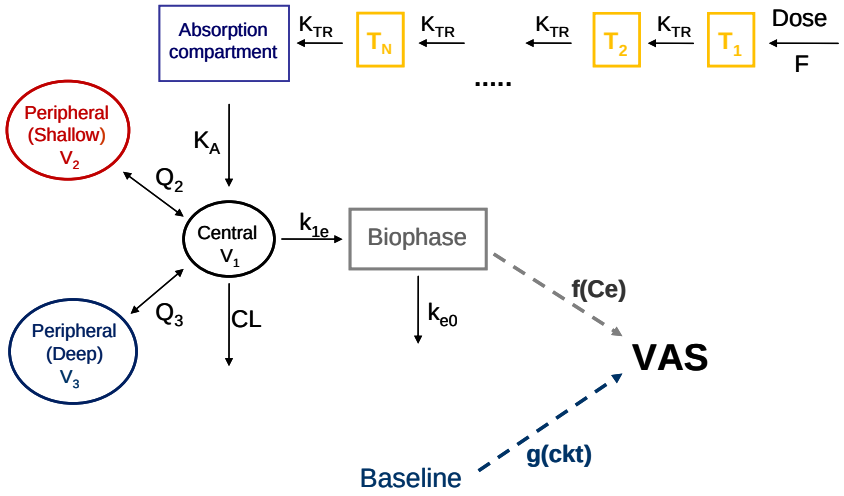

Fig. 1 Schematic representation of the PK/PD model used to describe the effects of flibanserin on VAS response. F; absolute bioavailability; $T_{1..N}$, transit compartments; k_{TR}, 1st order rate constant of transit; k_A, 1st order rate constant of absorption; V_1, V_2, V_3, apparent volumes of distribution of the central, peripheral shallow and peripheral deep compartments, respectively; CL_{D2}, CL_{D3}, inter-compartmental clearances; CL, total plasma clearance; k_{1e}, 1st order rate constant of distribution from the central compartment to the biophase compartment (using the effect compartment model its estimation is not required); k_{e0}, 1st order rate of elimination from the biophase; C_e, predicted effect site concentration; ckt, clock time; f(Ce), pharmacodynamic model, g(ckt), baseline model.

effects were ignored. Further model improvements were obtained when C_P was substituted by C_e, and when a sigmoidicity factor was introduced in the effect *vs.* C_e relationship. With the drug effect added, ISV remained significant for each of the height parameters of the baseline model, and it was found to be necessary to account for ISV in C_{50}. Covariance between ISV and the presence of IOV were not supported by the data ($p>0.05$). Sex did not significantly influence any of the baseline and drug effect parameters ($p>0.05$). Residual variability was described by an additive random-effect model on the logarithmic scale. Table III lists the PD parameter estimates of the population PK/PD model. ε-shrinkage was 5.75%, and η-shrinkage corresponding to $H_{6.65}$, $H_{10.77}$, $H_{21.1}$, and C_{50} was 13, 6.6, 5.7, and 12.1%, respectively. All parameters were estimated with adequate precision. Results from the bootstrap analyses provided median values of the parameters that were very close to the NONMEM estimates and the 95% confidence intervals did not include the value of zero for any of the parameters in the model. The results shown in Fig. 3

Table I Population Pharmacokinetic Parameter Estimates

			Bootstrap analysis (500 replicates) Median [2.5th–97.5th percentiles]	
Parameter	Estimate (RSE%)	ISV (RSE%)	Estimate	ISV
k_A (h^{-1})	1.61 (1.9)	52 (34)	1.62 [1.25–2.05]	51 [31–68]
F (%)	45.9 (2)	–	46 [39–53]	–
MTT (h)	0.41 (3.2)	47 (30)	0.42 [0.34–0.49]	46 [31–61]
NTC	16.4 (11.1)	94 (34)	16.2 [10.2–22.7]	88 [55–114]
V_1 (L)	13.1 (2.3)	–	13.0 [12.0–13.9]	–
CL (Lxh^{-1})	23.5 (2.5)	36 (20)	23.7 [21.5–25.7]	36 [28–43]
V_2 (L)	141 (2)	47 (24)	142 [120–169]	46 [33–58]
CL_{D2} (Lxh^{-1})	20.7 (4.3)	72 (23)	20.8 [17.1–25.7]	71 [52–86]
V_3 (L)	58.5 (4.9)	–	58.6 [51.7–67.0]	–
CL_{D3} (Lxh^{-1})	90.0 (3.6)	–	90.6 [82.3–99.0]	–
Residual error log(ng/mL)	0.13 (12)	–	0.13 [0.12–0.15]	–

Estimates are listed together with their corresponding relative standard error (RSE%); ISV, inter-subject variability expressed as coefficient of variation (%). k_A, 1st order rate constant of absorption; F, absolute bioavailability; MTT, mean transit time; NTC, number of transit compartments; V_1, V_2, V_3, apparent volumes of distribution of the central, shallow peripheral, and deep peripheral compartments, respectively; CL, total plasma clearance; CL_{D2}, CL_{D3}, inter-compartmental clearances between the shallow and deep peripheral compartments and the central compartment, respectively

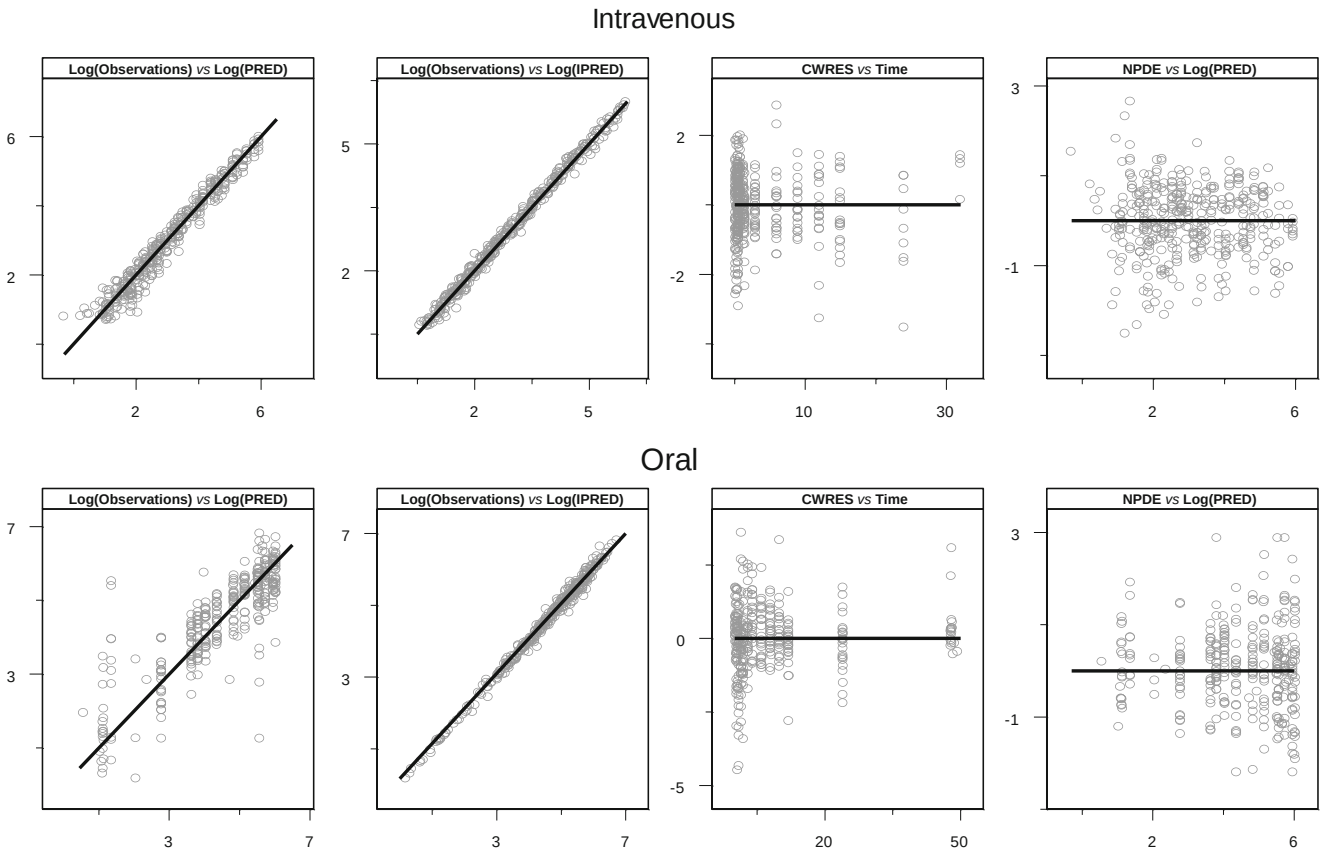

Fig. 2 Goodness of fit plots corresponding to the population PK model. PRED, population model predictions; IPRED, individual model predictions; CWRES, conditional weighted residuals; NPDE, normalized prediction distribution errors. Solid lines show the identity lines (*left panels*) and CWRES and NPDE = 0 (*right panels*).

(goodness of fit plots also showing NPDE) indicate that the model was supported by the data. Similar results were obtained from the NPC (see Table IV). The three descriptors ($VAS_{MAX\_Day\ 1}$, $VAS_{MAX\_Day\ 2}$, and% ΔVAS>2 cm) calculated from the raw data fell within the 90% prediction intervals calculated from the simulated studies. Based on the results from model evaluation it can be concluded that the selected model describes the raw data well.

Figure 4 allows the comparison of the observed data with the performance of the PK/PD model on an individual level. Taking into account the scattered nature of the data, the model overall provides a good description of the individual profiles.

Table II Results from the Numerical Predictive Check Corresponding to the Selected Population Pharmacokinetic Model

Formulation	Dose (mg)	C_{MAX} (ng/mL)		AUC_{last} (h × ng/mL)	
		Raw	Simulated	Raw	Simulated
Immediate release	100	413	426 [374–478]	2180	1938.2 [1706.4–2235.0]
Intravenous	0.5	9.7	9.5 [8.0–10.9]	5.5	6.9 [5.8–8.3]
	1	19.4	18.9 [16.1–21.9]	15.6	16.9 [14.4–19.8]
	2	41	38.1 [31.6–44.1]	45.5	49.6 [40.3–60.7]
	5	105	94.7 [77.0–111.2]	171.9	175.8 [133.2–221.8]
	10	196	189.6 [158.6–218.7]	319.2	354.9 [279.6–449.7]
	20	335	379.2 [318.9–436.3]	686	795.1 [595.9–1017.2]

Results are shown as median (raw data) and median [5th–95th percentiles] (simulations). C_{MAX}, maximum concentration of flibanserin in plasma, AUC_{last}, are under the plasma drug concentration *versus* time curve between 0 and last time of measurement

Table III Population Pharmacodynamic Parameter Estimates

			Bootstrap analysis (500 replicates) Median [2.5th–97.5th percentiles]	
Parameter	Estimate (RSE%)	ISV (RSE%)	Estimate	ISV
H_{0th} (cm)	2.01 (21)	21 (42)	2 [1.1–3.04]	28 [18–40]
H_{50th} (cm)	0.63 (31)	10 (40)	0.65 [0.32–1.1]	7 [6–8]
H_{100th} (cm)	1.01 (22)	11 (28)	1.01 [0.62–1.6]	11 [8–14]
k_{e0} (h^{-1})	2.24 (27)	–	2.6 [1.5–5.15]	–
C_{50} (ng/mL)	306 (13)	43 (43)	317 [250–427]	42 [22–60]
γ	5.21 (23)	–	5.2 [3.35–7.32]	–
Residual error [log(cm)]	0.78 (18)	–	0.71 [0.65–0.91]	–

Estimates are listed together with their corresponding relative standard error (RSE%); ISV, inter-subject variability expressed as coefficient of variation (%). $H_{0–100th}$, Height of breakpoints at 6.65, 10.77, and 21.1 h clock time, respectively; k_{e0}, first order rate constant of elimination from the effect compartment; C_{50}, effect site concentration (C_e) eliciting half of maximum attainable VAS response; γ, parameter governing the steepness of the VAS *vs.* C_e relationship

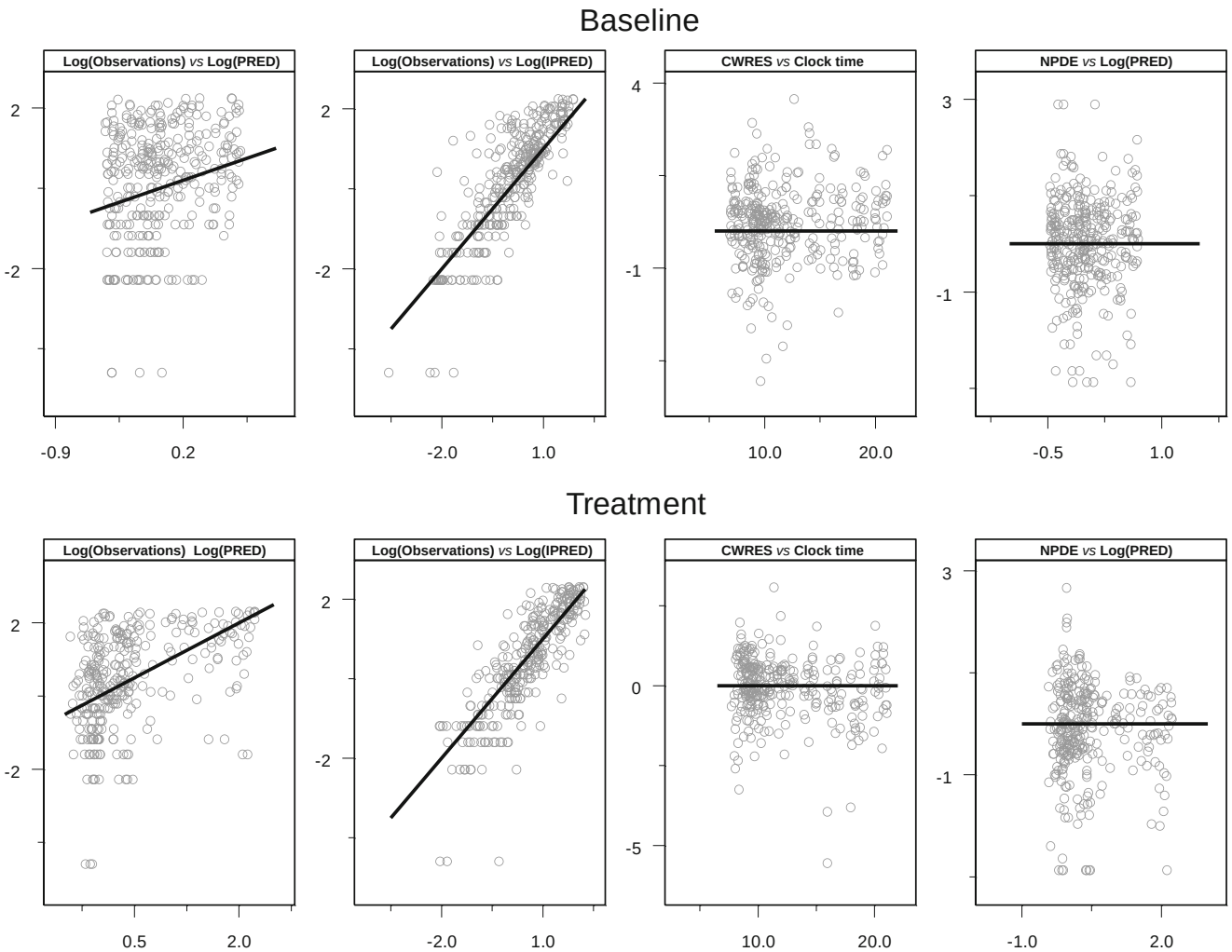

Fig. 3 Goodness of fit plots corresponding to the population PK/PD model. PRED, population model predictions; IPRED, individual model predictions; CWRES, conditional weighted residuals; NPDE, normalized prediction distribution errors. Solid lines show the identity lines (*left panels*) and CWRES and NPDE = 0 (*right panels*).

Table IV Results from the Numerical Predictive Check Corresponding to the Selected Population Pharmacokinetic/Pharmacodynamic Model

	Raw	Simulated
$VAS_{MAX\_Day\ 1}$ (cm)	5.05	5.6 [4.5–6.6]
$VAS_{MAX\_Day\ 2}$ (cm)	6.95	6.99 [6.1–7.8]
% ΔVAS>2 cm (%)	25	37 [21–56]

Results are shown as median (raw data) and median [5th–95th percentile] (simulations). $VAS_{MAX\_Day\ 1}$ (cm), Maximum VAS score at day 1 (no treatment day); $VAS_{MAX\_Day\ 2}$ (cm), Maximum VAS score at day 2 (treatment day);% ΔVAS>2 cm, percentage of subjects showing a difference greater than 2 cm in the maximum increment in VAS response between day 2 and day1

The population's typical concentration- and VAS profiles predicted by the model are visualized in Fig. 5. The typical profiles of flibanserin plasma concentrations in the central compartment and in the effect compartment are quite similar (left panel). The model predicted typical values of C_{MAX} and maximum C_e of 417 and 324 ng/mL at 45 and 90 min after administration, respectively. The steepness of the VAS *vs.* C_e relationship as shown in the middle panel supports the concept of a threshold C_e concentration (~200 ng/mL) below which the flibanserin concentration has hardly any impact on the drowsiness effect. The VAS *vs.* clock time profile at baseline and after administration of a single oral dose of 100 mg flibanserin is represented in the right panel: a typical VAS increase of approximately 4 cm is predicted for a baseline VAS score of 2 cm that reaches its maximum within the first 2 h after drug administration and returns to baseline values 4 h after administration.

Model Simulations

Figure 6 shows the distribution of the percentages of subjects with a difference greater than 2 cm in the maximum increment in VAS response between baseline and treatment day for different hypothetical maximum flibanserin plasma concentrations resulting from different absorption rates.

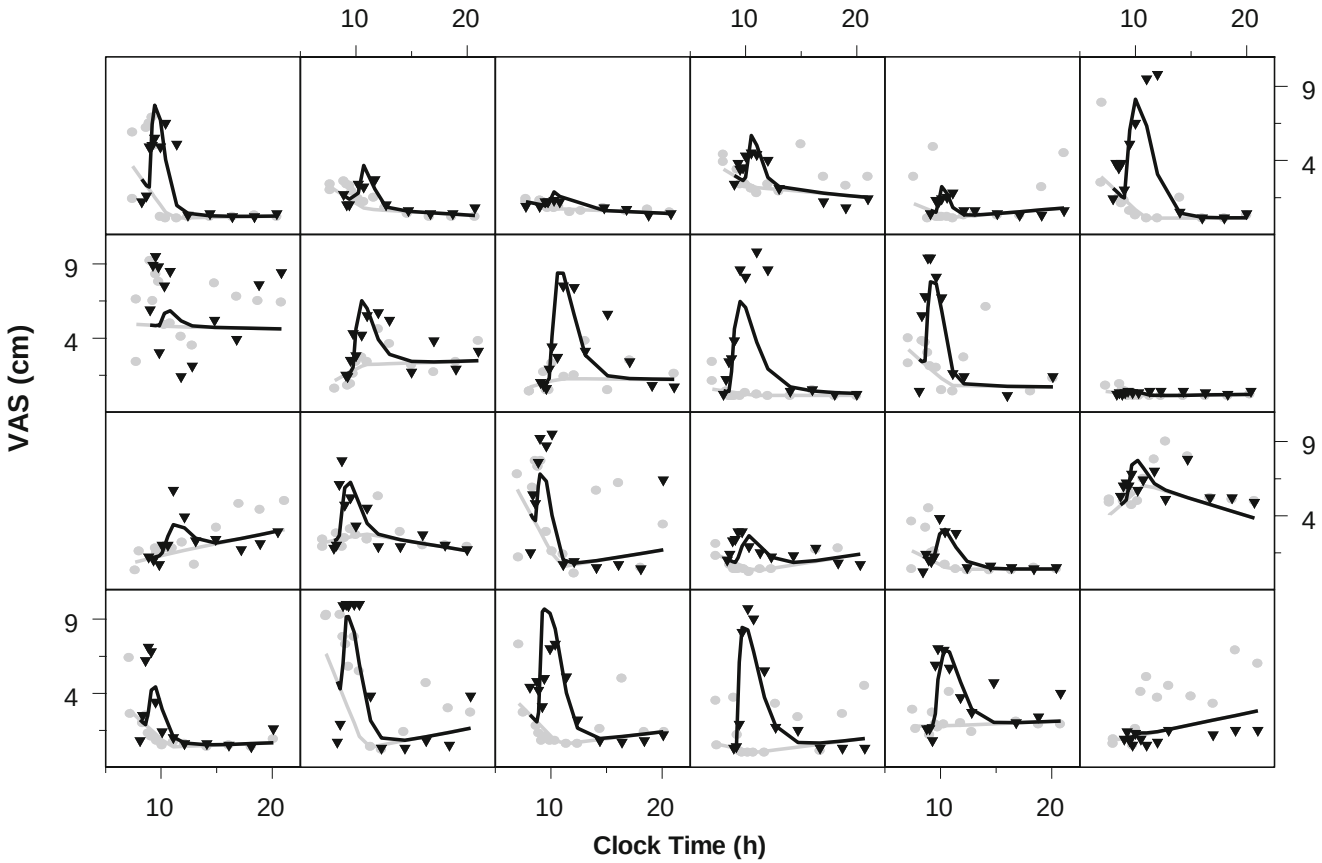

Fig. 4 Comparison of individual observed VAS response values (*grey circles*, baseline day; *black triangles*, treatment day) and individual model predictions (*grey line*, baseline day; *black line*, treatment day).

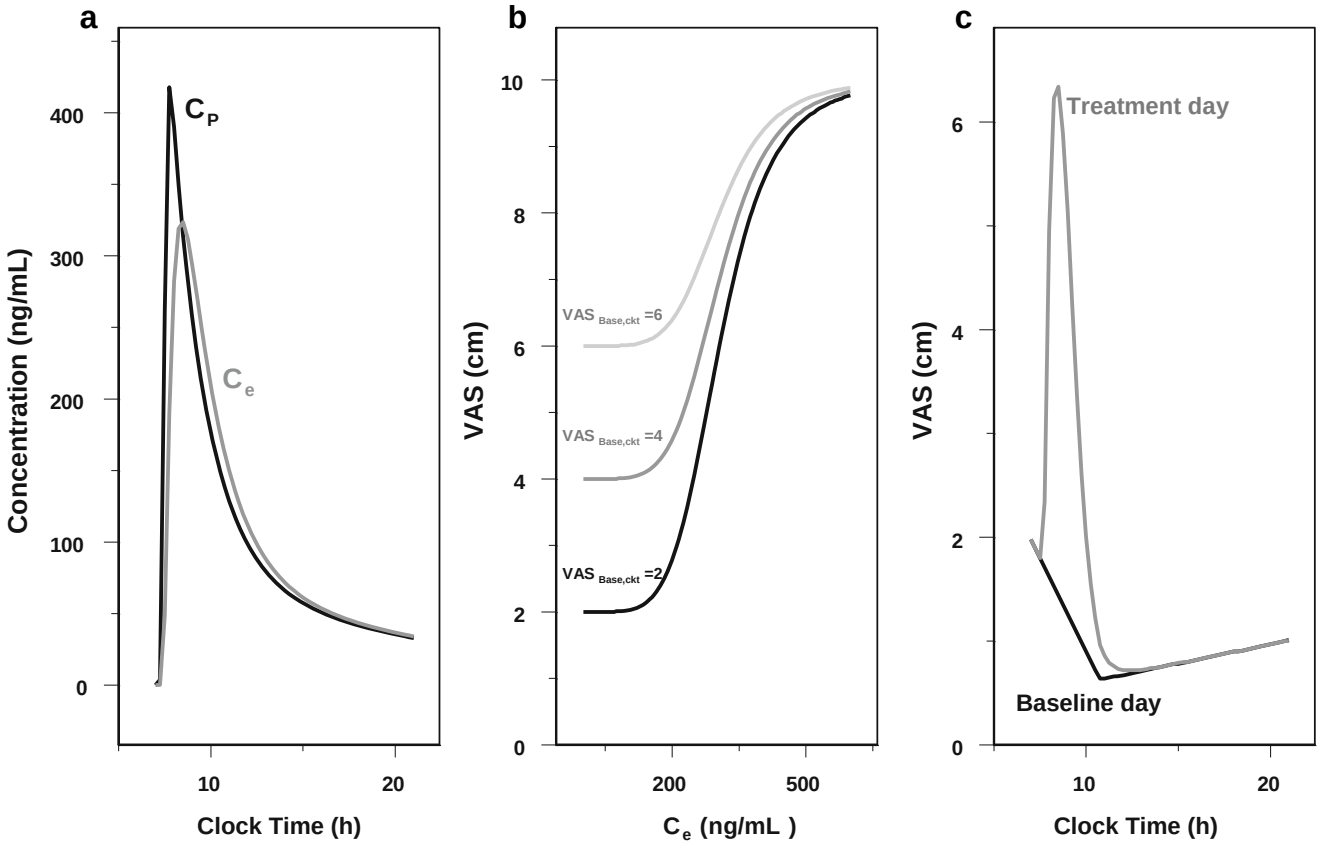

Fig. 5 (**a**) Typical predicted plasma and effect concentrations time profiles after a 100 mg oral dose of flibanserin. (**b**) Typical predicted pharmacodynamic profiles for baseline VAS scores of 2, 4, and 6 cm. (**c**) Typical predicted VAS profile over time after administration of a single oral dose of 100 mg flibanserin (*black*, baseline day; *grey*, treatment day).

DISCUSSION

In this study a population PK/PD model for the drowsiness effects of flibanserin in healthy volunteers was developed. The various evaluation methods applied to the PK and the PK/PD model underlined successfully the ability of the model to describe the data comprehensively.

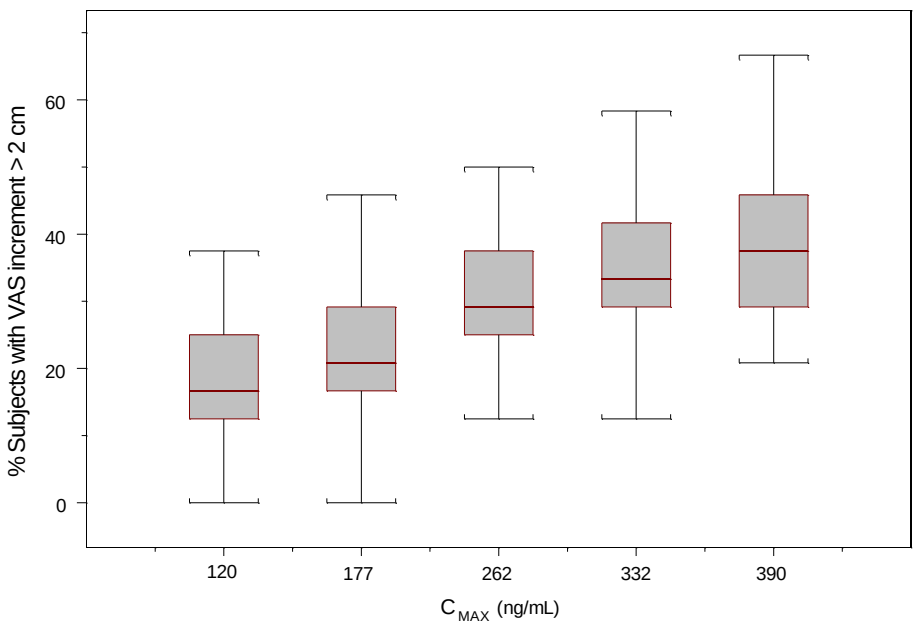

Fig. 6 Relationship between percentage of subjects showing a difference greater than 2 cm in the maximum increment in VAS response between treatment day and baseline day *vs.* C_{MAX}. C_{MAX} values represent the median maximum plasma concentrations calculated from 500 simulated studies.

Flibanserin showed similar PK characteristics between males and females and linear PK characteristics in the dose range studied. Population estimates of CL, V (calculated as the sum of V_1, V_2, and V_3, the apparent volumes of distribution of the central, and shallow and deep peripheral compartments, respectively) and F were 23.5 L h^{-1}, 212.6 L and 46%, respectively. These values were similar to values obtained from previous studies by non-compartmental analysis, 26 L h^{-1}, 186 L, and 33%, respectively (7). After oral administration flibanserin was quickly absorbed. Once the drug was released from the tablet, 46% of the absorbed dose reached the systemic circulation in approximately 25 min, and maximum concentration in plasma occurred 45 min after drug administration. Inter-subject variability in the processes representing the latency period during absorption was high while inter-subject variability in total drug exposure represented by CL was moderate (36%).The analysis of the time course of the VAS effects revealed that there was a small but significant delay in the kinetic profiles of flibanserin between the central compartment and the effect site, that was accounted for by introducing an effect compartment model (17). The derived value for the half-life of elimination of the effect compartment was short (approximate 18 min) indicating that plasma and effect site concentrations are rapidly in equilibrium. Although the distribution delay between central compartment and effect site was small, the model including the effect compartment resulted in a better description of the response *vs* time profiles. Although it is well known that there is a circadian rhythm in day-time alertness which also varies significantly between individuals and occasions (20), the observed high variability in the magnitude of VAS and in the time trends between subjects precluded the identification of clear patterns, and represented a challenge for the description of the time course of VAS at baseline and for extracting the drowsiness effects of flibanserin. Linear splines have often been used to describe complex drug absorption profiles (21), or transient experimentally induced changes in baseline response (22). Given the variability shown in the data and the subjective nature of the measurements, some degree of IOV was expected, however could not be accounted for, probably due to the fact that only measurements from one baseline day were used. The model used to constrain the predicted VAS score has been applied several times in the analysis of continuous data as in case of the IIEF domain in erectile dysfunction (23), VAS pain rating (24), and PANSS scores in schizophrenia (25). The model was adequate to describe the data taking into account that none of the observed VAS score achieved the maximum of 10 cm. In case individuals reporting frequently maximum VAS scores, which was not the case here, other approaches considering maximum response as censored observation might represent a better alternative (26,27).The PK/PD model established in the present study has been built with VAS data obtained after a single oral administration of the proposed therapeutic dose of flibanserin for the treatment of hypoactive sexual desire disorder in premenopausal women. As female HSDD patients generally present with good physical health, this model, although established based on healthy volunteer data, may serve as a good basis for further investigations of drowsiness over time in the target population.

The model developed in the current analysis has potential applications as the occurrence of acute sedative side effects of flibanserin can be predicted in situations where the plasma concentration-time profile of flibanserin and especially maximum flibanserin plasma concentrations are altered, e.g. due to concomitant disease or medication or due formulation changes (Fig. 6). However it has to be recognized that the model describing drowsiness over time is highly empirical. One of its limitations is that two breakpoints are located at the time of the first and last measurements. However such characteristic will not limit its applicability of simulating different clinical scenarios since the drug administration and measurements times used in the current trial can be considered very standard and likely to be used in further studies. It has to be taken into consideration that the model was developed based on single dose data and therefore inference to multiple dosing should be done with caution.

To summarize, a population PK/PD model for the VAS drowsiness effect of flibanserin has been developed from data obtained in healthy female and male volunteers. A rapid distribution from the central to the effect compartment has been identified. The VAS *vs.* C_e relationship was very steep, suggesting that at C_e lower than ~200 ng/mL that are reached approximately 4 h after administration, flibanserin exerts a relatively small effect on drowsiness as measured by the VAS scale.

ACKNOWLEDGMENTS & DISCLOSURES

Iñaki F. Trocóniz has received financial research support from Boehringer Ingelheim Pharma GmbH & Co KG. Katja Boland and Alexander Staab are employees of Boehringer Ingelheim Pharma GmbH & Co KG.

REFERENCES

1. American Psychiatric Association. DSM-IV: Diagnostic and statistical manual f mental disorders, 4th edition. Text revision. Washington: American Psychiatric Press; 2000.
2. Shifren JL, Monz BU, Russo PA, Segreti A, Johannes CB. Sexual problems and distress in United States women: prevalence and correlates. Obstet Gynecol. 2008;112(5):970–8.

3. Invernizzi RW, Sacchetti G, Parini S, Acconcia S, Samanin R. Flibanserin, a potential antidepressant drug, lowers 5-HT and raises dopamine and noradrenaline in the rat prefrontal cortex dialysate: role of 5-HT(1A) receptors. Br J Pharmacol. 2003;139(7):1281–8.
4. Kennedy S. Flibanserin: initial evidence of efficacy on sexual dysfunction, in patients with major depressive disorder. J Sex Med. 2010;7(10):3449–59.
5. Ferger B, Shimasaki M, Ceci A, Ittrich C, Allers KA, Sommer B. Flibanserin, a drug intended for treatment of hypoactive sexual desire disorder in pre-menopausal women, affects spontaneous motor activity and brain neurochemistry in female rats. Naunyn Schmiedebergs Arch Pharmacol. 2010;381(6):573–9.
6. Newman-Tancredi A, Heusler P, Martel JC, Ormière AM, Leduc N, Cussac D. Agonist and antagonist properties of antipsychotics at human dopamine D4.4 receptors: G-protein activation and K+ channel modulation in transfected cells. Int J Neuropsychopharmacol. 2008;11(3):293–307.
7. Boehringer Ingelheim. Briefing document, Flibanserin Tablet, NDA 22-526 Reproductive Health Drugs Advisory Committee Meeting, June 18, 2010. Available from:http://www.fda.gov/downloads/AdvisoryCommittees/CommitteesMeetingMaterials/Drugs/ReproductiveHealthDrugsAdvisoryCommittee/UCM215438.pdf
8. NONMEM Users Guides. Beal SL, Sheiner LB, Boeckmann AJ, editors. Icon Development Solutions, Ellicott City, Maryland, USA; 1989–2006.
9. Karlsson MO, Sheiner LB. The importance of modeling interoccasion variability in population pharmacokinetic analyses. J Pharmacokinet Biopharm. 1993;21(6):735–50.
10. Hooker AC, Staatz CE, Karlsson MO. Conditional weighted residuals (CWRES): a model diagnostic for the FOCE method. Pharm Res. 2007;24(12):2187–97.
11. Ludden TM, Beal SL, Sheiner LB. Comparison of the Akaike Information Criterion, the Schwarz criterion and the F test as guides to model selection. J Pharmacokinet Biopharm. 1994;22(5):431–45.
12. Lindbom L, Ribbing J, Jonsson EN. Perl-speaks-NONMEM (PsN)—a Perl module for NONMEM related programming. Comput Methods Programs Biomed. 2004;75(2):85–94.
13. Comets E, Brendel K, Mentré F. Computing normalised prediction distribution errors to evaluate nonlinear mixed-effect models: the npde add-on package for R. Comput Methods Programs Biomed. 2008;90(2):154–66.
14. Holford NH, Ambros RJ, Stoeckel K. Models for describing absorption rate and estimating extent of bioavailability: application to cefetamet pivoxil. J Pharmacokinet Biopharm. 1992;20(5):421–42.
15. Savic RM, Jonker DM, Kerbusch T, Karlsson MO. Implementation of a transit compartment model for describing drug absorption in pharmacokinetic studies. J Pharmacokinet Pharmacodyn. 2007;34(5):711–26.
16. DeBoor. A practical guide to splines. New York: Springer Verlag; 1998.
17. Sheiner LB, Stanski DR, Vozeh S, Miller RD, Ham J. Simultaneous modeling of pharmacokinetics and pharmacodynamics: application to d-tubocurarine. Clin Pharmacol Ther. 1979;25(3):358–71.
18. Ostelo RW, Deyo RA, Stratford P, Waddell G, Croft P, Von Korff M, *et al.* Interpreting change scores for pain and functional status in low back pain: towards international consensus regarding minimal important change. Spine (Phila Pa 1976). 2008;33(1):90–4.
19. Karlsson MO, Savic RM. Diagnosing model diagnostics. Clin Pharmacol Ther. 2007;82(1):17–20.
20. Van Dongen HPA, Dinges DF. Circadian rhythm in sleepiness, alertness and performance. In: Kryger MH, Roth T, Dement WC, editors. Principles and practice of sleep medicine. 4th ed. Philadelphia: Saunders; 2005. p. 435–43.
21. Drover DR, Angst MS, Valle M, Ramaswamy B, Naidu S, Stanski DR, *et al.* Input characteristics and bioavailability after administration of immediate and a new extended-release formulation of hydromorphone in healthy volunteers. Anesthesiology. 2002;97(4):827–36.
22. Josa M, Urizar JP, Rapado J, Dios-Viéitez C, Castañeda-Hernández G, Flores-Murrieta F, *et al.* Pharmacokinetic/pharmacodynamic modeling of antipyretic and anti-inflammatory effects of naproxen in the rat. J Pharmacol Exp Ther. 2001;297(1):198–205.
23. Staab A, Tillmann C, Forgue ST, Mackie A, Allerheiligen SR, Rapado J, *et al.* Population dose–response model for tadalafil in the treatment of male erectile dysfunction. Pharm Res. 2004;21(8):1463–70.
24. Kshirsagar S, Gear R, Levine J, Verotta D. A mechanistic model for the sex-specific response to nalbuphine and naloxone in postoperative pain. J Pharmacokinet Pharmacodyn. 2008;35(1):69–83.
25. Ortega I, Perez-Ruixo JJ, Stuyckens K, Piotrovsky V, Vermeulen A. Modeling the effectiveness of paliperidone ER and olanzapine in schizophrenia: meta-analysis of 3 randomized, controlled clinical trials. J Clin Pharmacol. 2010;50(3):293–310.
26. Luks AM, Zwass MS, Brown RC, Lau M, Chari G, Fisher DM. Opioid-induced analgesia in neonatal dogs: pharmacodynamic differences between morphine and fentanyl. J Pharmacol Exp Ther. 1998;284(1):136–41.
27. Garrido MJ, Valle M, Campanero MA, Calvo R, Trocóniz IF. Modeling of the *in vivo* antinociceptive interaction between an opioid agonist, (+)-O-desmethyltramadol, and a monoamine reuptake inhibitor, (−)-O-desmethyltramadol, in rats. J Pharmacol Exp Ther. 2000;295(1):352–9.